

© 2013 AIP Publishing LLC. All rights reserved. Access to this work was provided by the University of Maryland, Baltimore County (UMBC) ScholarWorks@UMBC digital repository on the Maryland Shared Open Access (MD-SOAR) platform.

Please provide feedback

Please support the ScholarWorks@UMBC repository by emailing [scholarworks-group@umbc.edu](mailto:scholarworks-group@umbc.edu) and telling us what having access to this work means to you and why it's important to you. Thank you.

# Plasmonic nanoparticles and metasurfaces to realize Fano spectra at ultraviolet wavelengths

Cite as: Appl. Phys. Lett. **103**, 143113 (2013); <https://doi.org/10.1063/1.4823575>

Submitted: 03 May 2013 . Accepted: 13 September 2013 . Published Online: 01 October 2013

Christos Argyropoulos, Francesco Monticone, Giuseppe D'Aguanno, and Andrea Alù



View Online



Export Citation



CrossMark

## ARTICLES YOU MAY BE INTERESTED IN

[Experimental realization and modeling of a subwavelength frequency-selective plasmonic metasurface](#)

Applied Physics Letters **99**, 221106 (2011); <https://doi.org/10.1063/1.3664634>

[Near-field imaging of spin-locked edge states in all-dielectric topological metasurfaces](#)

Applied Physics Letters **114**, 031103 (2019); <https://doi.org/10.1063/1.5055601>

[Optical metasurfaces with robust angular response on flexible substrates](#)

Applied Physics Letters **99**, 163110 (2011); <https://doi.org/10.1063/1.3655332>

Lock-in Amplifiers  
up to 600 MHz



# Plasmonic nanoparticles and metasurfaces to realize Fano spectra at ultraviolet wavelengths

Christos Argyropoulos,<sup>1</sup> Francesco Monticone,<sup>1</sup> Giuseppe D'Aguanno,<sup>2</sup> and Andrea Alù<sup>1,a)</sup>

<sup>1</sup>Department of Electrical and Computer Engineering, The University of Texas at Austin, Austin, Texas 78712, USA

<sup>2</sup>Aegis Technologies, Nanogenesis Division, 410 Jan Davis Dr., Huntsville, Alabama 35806, USA

(Received 3 May 2013; accepted 13 September 2013; published online 1 October 2013)

We discuss the possibility to realize sharp Fano scattering signatures in the ultraviolet (UV) range, based on dipolar scattering of nanoparticles. At these frequencies, material losses usually do not allow sharp resonant effects, hindering plasmonic applications based on higher-order multipolar modes, like conventional Fano resonances. We propose to excite degenerate scattering states supported by core-shell nanoparticles made of a sapphire core and an aluminum shell. We predict enhanced, highly confined fields, supporting sharp far-field scattering signatures from single nanoparticles and planar arrays of them. These results may lead to the design of UV filters, photodetectors, sensors, and energy-harvesting devices. © 2013 AIP Publishing LLC. [<http://dx.doi.org/10.1063/1.4823575>]

Significant research efforts have been recently dedicated to enhancing and engineering the interaction of light and matter at subwavelength dimensions. This interest has fostered the growth of the recent research field of plasmonics, demonstrating great potential towards combining the miniaturized dimensions of semiconductor electronic technology with the large data rates and enhanced bandwidth performances achieved by photonic devices.<sup>1</sup> Exciting applications have been envisioned based on the strong confinement of light in deeply subwavelength dimensions.<sup>2</sup> One of the most interesting effects enabled by plasmonics is the ultra-sharp Fano resonant scattering response supported by metallic nanostructures at optical and infrared (IR) frequencies.<sup>3–7</sup> These asymmetric resonances are usually based on the interaction between dipolar bright modes with higher-order, more narrowband dark modes.<sup>3</sup> Their characteristics have shown great benefits in various scenarios, in particular, for optical filtering, sensing, lasing, and slow-light applications.

The involvement of higher-order modes (quadrupoles, octupoles, etc.) leads to enhanced stored energy in the plasmonic device, which translates into higher sensitivity to the Ohmic losses typical of metals at optical frequencies. Furthermore, conventional plasmonic Fano resonances, arising from the interference between two different scattering orders, can be usually observed only over a portion of the angular spectrum due to interference. Recently, it was proposed that similarly sharp Fano-like resonant signatures can be obtained by the interaction of purely dipolar modes.<sup>8–13</sup> In our recent works, we showed that this possibility may be controlled by closely coupling in the frequency spectrum *cloaking* and *resonant* states of a symmetric and isotropic nanoparticle. In this case, a dipole-dipole Fano-like response can be observed for all angles of incidence and in the total scattering cross section (SCS), even for a single nanoparticle. Moreover, enhanced fields are obtained at this sharp dipolar

resonance, strongly confined at the core of the nanoparticle, all across the Fano spectrum. Depending on how these states are excited, these resonant phenomena may be made more or less sensitive to the background medium and the core material,<sup>12</sup> providing an unprecedented flexibility to realize different functionalities. A plethora of applications has been envisioned from these plasmonic structures, such as robust sensors,<sup>11</sup> nano-biomarkers<sup>12</sup> and efficient nonlinear all-optical switches.<sup>10</sup>

Until now, the most common materials considered for plasmonic applications have been silver, copper, and gold, because they can sustain efficient excitation of both propagating and localized surface plasmons at optical frequencies. However, they suffer from inherent disadvantages, such as increased losses, high cost, and low abundance on Earth,<sup>13</sup> which set severe limitations towards the future commercial applications and mass-production of plasmonic devices based on these materials. Alternatively, it was demonstrated that efficient plasmon excitation combined with relatively low losses can also be sustained at mid-infrared frequencies using doped semiconductor materials.<sup>12,14,15</sup>

Comparatively, less research attention has been dedicated to plasmonic effects occurring at very high frequencies, such as in the ultraviolet (UV) spectrum. This is mainly because the aforementioned noble metals and semiconductors have lower plasma frequencies compared to the UV frequency range and, as a result, they are mostly transparent and do not exhibit plasmonic behavior in such regimes. Aluminum (Al) is the ideal material to sustain surface plasmons at UV wavelengths, due to its high plasma frequency ( $\sim 15$  eV or  $\lambda = 85$  nm). In addition, Al is the third most abundant element on Earth, which makes it cheap and ideal for mass-production. Interesting and diverse applications have been recently envisioned at UV frequencies based on Al plasmonic devices, such as boosted nonlinear operations,<sup>16</sup> efficient surface-enhanced Raman scattering (SERS) substrates,<sup>17,18</sup> plasmonic nanoantennas,<sup>19</sup> enhanced fluorescence,<sup>20,21</sup> extraordinary optical transmission gratings,<sup>22,23</sup> and energy harvesting devices.<sup>24</sup>

<sup>a)</sup> Author to whom correspondence should be addressed. Electronic mail: [alu@mail.utexas.edu](mailto:alu@mail.utexas.edu)

Less attention has been paid to plasmonic structures exhibiting Fano resonances at UV frequencies, which may be used, for instance, as sharp solar blinds to isolate portions of the UV frequency spectrum, while transmitting optical radiation, or as sensitive nanosensors and photodetectors. The reason for the comparatively less amount of research on this topic is the larger loss factor of Al in the UV compared to other noble metals at lower frequencies, which hinders higher-order resonances on which conventional Fano responses are based. In this letter, we explore the possibility to induce dipole-dipole plasmonic Fano resonances at UV frequencies supported by properly engineered core-shell subwavelength nanoparticles, similar to the concept proposed in Ref. 10 for operation in the visible. The proposed geometry, shown in the inset of Fig. 1(b), is composed of a sapphire ( $\text{Al}_2\text{O}_3$ ) dielectric core with radius  $a_c$  surrounded by a metallic shell made of aluminum with radius  $a$ . According to the theory presented in Refs. 10–12 for thick, subwavelength plasmonic shells, the electric dipolar response of this nanoparticle can present an ultrasharp degenerate resonant state when  $\epsilon_{\text{Al}} = -\epsilon_{\text{Al}_2\text{O}_3}/2$ . Under this condition, the frequency dispersion of a cloaking (dark) state merges with the one of a resonant (bright) state, producing an asymmetric Fano-type resonance in the scattering spectrum. Since the two interfering states are associated with the same dipolar scattering mode, we are able to realize an asymmetric, sharp Fano-resonant scattering signature with a single, isotropic, and center-symmetric subwavelength scatterer.

The scattering performance of the proposed nanoparticle is quantitatively analyzed using the well-established Mie scattering theory.<sup>25</sup> Realistic losses are considered for both Al and  $\text{Al}_2\text{O}_3$ , their permittivity values are obtained from experimental data<sup>26</sup> and the nanoparticle is embedded in free space. The normalized SCS of a subwavelength core-shell nanosphere with inner layer radius  $a_c = 3$  nm and outer radius  $a = 8.5$  nm is computed and plotted in Fig. 1(a). Interestingly, the normalized SCS can go from  $-13$  dB [point I in Fig. 1(a)] to almost  $-30$  dB [point II in Fig. 1(a)] in a narrow wavelength range. Note that this sharp Fano resonant linewidth is obtained at deep-UV frequencies, where most metals are actually semi-transparent, while dielectric nanoparticles do not generally show peculiar scattering signatures because dielectric materials are opaque in this

wavelength range, due to their largely increased absorption around the interband transitions. Realistic losses of plasmonic and dielectric materials have been fully taken into account in our calculations, accurately reflecting the response of a realistic structure implementable within current nanofabrication techniques.

The inset of Fig. 1(a) shows two snapshots in time of the  $E_x$  field component at the high scattering point I (resonance) and low scattering point II (cloaking). Enhanced and strongly confined fields are obtained inside the composite nanoparticle for both resonant and cloaking states. In contrast, outside the core-shell particle, the fields are dramatically different across the linewidth of the UV Fano resonance. In the resonant state (point I), large scattering efficiency is observed, similar to ordinary dipolar plasmonic resonances supported by silver or gold nanoparticles at optical frequencies.<sup>2</sup> Conversely, in the cloaking state (point II), the impinging fields travel around the scatterer almost unperturbed, similar to scattering cancellation designs proposed in Refs. 27 and 28. It is interesting that such strong variation of the field distribution can be achieved over a narrow frequency range, which indicates a strong and peculiar interaction of the subwavelength nanoparticle with UV radiation. In Fig. 1(b) a cross-section of the field enhancement ( $|E|/|E_{\text{inc}}|$ ) is plotted along the  $x$ -axis crossing the center of the nanoparticle at the resonant (point I/red line) and cloaking (point II/blue line) wavelengths. Enhanced fields are obtained inside the plasmonic nanoparticle across the entire Fano spectrum shown in Fig. 1(a) and are strongly confined at the interface between the Al shell and the sapphire core. In this case, a strongly localized plasmon is formed, and the higher field enhancement at the metallic shell side observed in the figure can be explained by applying the boundary condition on the radial component of the electric displacement vector at this interface. Even at the cloaking frequency, significantly enhanced fields are observed in the core, which may be of interest to boost nonlinear effects at UV frequencies, as demonstrated for optical antennas<sup>29,30</sup> and epsilon-near-zero plasmonic waveguides<sup>31</sup> at optical frequencies. These features may lead to the design of low-intensity memories, switches, and sensitive tunable sensors at UV wavelengths.

Next, we check the effect of different dielectric background materials in the scattering response of the proposed

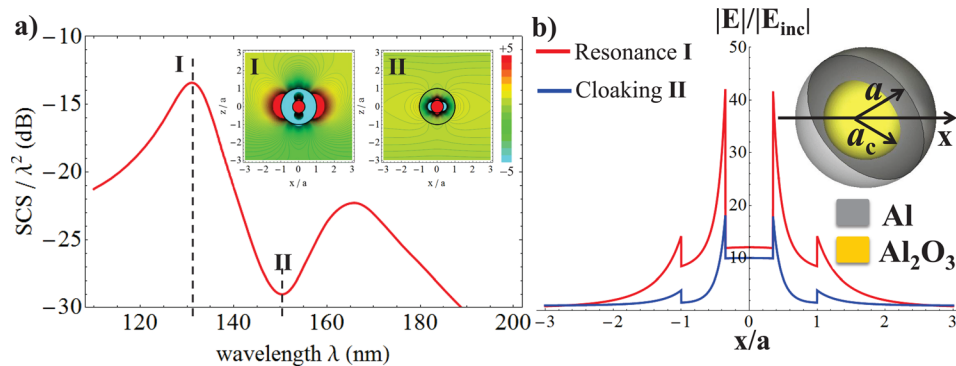


FIG. 1. (a) Normalized scattering cross section of the composite nanoparticle with geometry shown in the inset of panel (b). The radius of the core is  $a_c = 3$  nm and the outer layer radius is  $a = 8.5$  nm. The inset of (a) shows snapshots in time of the  $E_x$  field component at the resonance and cloaking wavelengths, denoted by I and II, respectively. (b) Field enhancement across the composite nanoparticle as a function of the normalized transverse direction ( $x/a$ ) at the resonant I (red line) and cloaking II (blue line) wavelengths.

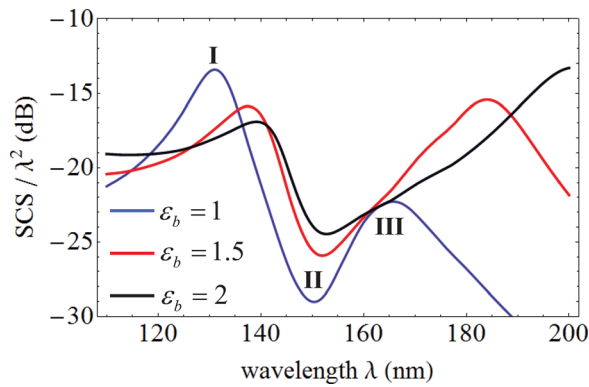


FIG. 2. Sensitivity of the UV Fano resonance to the permittivity  $\epsilon_b$  of the background medium. The nanoparticle has the same dimensions as in Fig. 1. The narrow resonance, cloaking, and broad dipolar resonance wavelengths are denoted by I, II, and III, respectively.

plasmonic nanoparticle. The UV Fano dispersion is plotted in Fig. 2 as a function of the surrounding medium permittivity. It is evident that the asymmetric Fano response is only slightly affected by variations of the background permittivity, which is consistent with the results presented in Ref. 12. The physical reason for this behavior is that the cloaking-resonance pair supporting the dipole-dipole UV Fano resonance is sustained by the localized plasmon residing at the inner spherical interface between the plasmonic (Al) shell and dielectric ( $\text{Al}_2\text{O}_3$ ) core. Hence, the peak (point I) and dip (point II) in the scattering response are almost insensitive to the background environment. On the contrary, the broad dipolar resonance at lower frequencies (point III in Fig. 2) is strongly affected by the background material.<sup>12</sup> As a result, the nanoparticles can be embedded in any host medium without significantly affecting the main features and robustness of this “built-in” UV Fano response, which may lead to, e.g., UV tagging applications.

In a realistic scenario, the ideal core-shell geometry that we have described would be modified upon exposure to ambient conditions, since the aluminum outer layer may oxidize and a thin native oxide  $\text{Al}_2\text{O}_3$  layer would form around the Al interface.<sup>32,33</sup> Here, we explore this issue and quantitatively assess the performance of the modified geometry, considering an additional thin layer (1.5 nm) of  $\text{Al}_2\text{O}_3$  around the plasmonic outer layer of the core-shell geometry of Fig. 1, as

shown in the inset of Fig. 3(b). The nanoparticle has now three layers and the dimensions are chosen to be: core radius  $a_{c1} = 3$  nm, middle plasmonic layer radius  $a_{c2} = 8.5$  nm (same dimensions as in Fig. 1 for a fair comparison), and outer layer radius  $a = 10$  nm. The calculated normalized SCS for this multilayered nanoparticle is shown in Fig. 3(a), demonstrating similarly sharp features in the UV range. As expected, the scattering excursions are slightly smaller, and the resonance bandwidth a bit broader compared to the previous case [see Fig. 1(a)], due mainly to the Ohmic losses of the sapphire outer layer, hence reducing the efficiency of plasmon excitation. However, a fairly sharp Fano response is still preserved. Also in this case we assumed a free-space background, but we expect the UV Fano resonance to be almost totally unaffected by a change in host medium, as shown in Fig. 2.

The fields are still confined inside the nanoparticle and strongly enhanced across the Fano resonance linewidth [Fig. 3(b)] when compared to the incident radiation, as shown in the field distributions in the inset of Fig. 3(a) at the wavelengths of the resonant (point I) and cloaking states (point II). The field enhancement is slightly lower compared to the two-layer case shown in Fig. 1(b), due to the additional thin outer layer of  $\text{Al}_2\text{O}_3$ , which strongly affects the surface plasmon localized at the outer spherical interface, as evident by a comparison of the field distributions in Figs. 1 and 3. However, high enhancement of the electric field is still obtained, especially at the interface between the Al shell and the  $\text{Al}_2\text{O}_3$  core, and the field level inside the core is almost the same as before. Note that the abrupt drop in field enhancement in the outer sapphire layer is mainly due to the high value of permittivity of  $\text{Al}_2\text{O}_3$  in this frequency region<sup>26</sup> and the continuity of the normal component of the electric displacement vector. These results demonstrate that narrow dipolar Fano resonant features and highly enhanced fields are preserved even after oxidization of the Al shells, which make the proposed composite plasmonic structure appealing for practical realizations and realistic applications.

The scattering signal obtained from an individual plasmonic nanoparticle is small in the far-field, due to its extremely subwavelength dimensions, and for practical purposes collections of such particles would be of more interest to form more complex nanodevices. For this reason, we

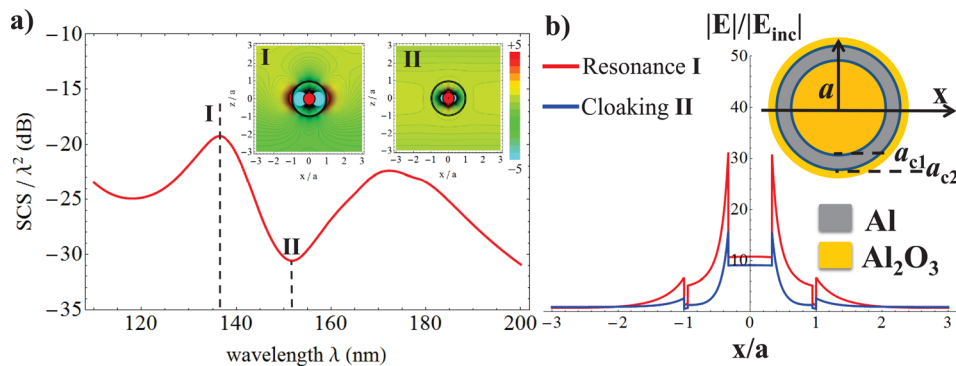


FIG. 3. (a) Normalized scattering cross section of the three-layer composite nanoparticle with geometry shown in the inset of panel (b). The radius of the core is  $a_{c1} = 3$  nm, the middle layer radius  $a_{c2} = 8.5$  nm, and the outer layer radius  $a = 10$  nm. The inset of (a) shows two snapshots in time of the  $E_x$  field component at the resonance and cloaking wavelengths, denoted by I and II, respectively. (b) Field enhancement across the three-layer composite nanoparticle as a function of the normalized transverse direction ( $x/a$ ) at the resonant I (red line) and cloaking II (blue line) wavelengths.



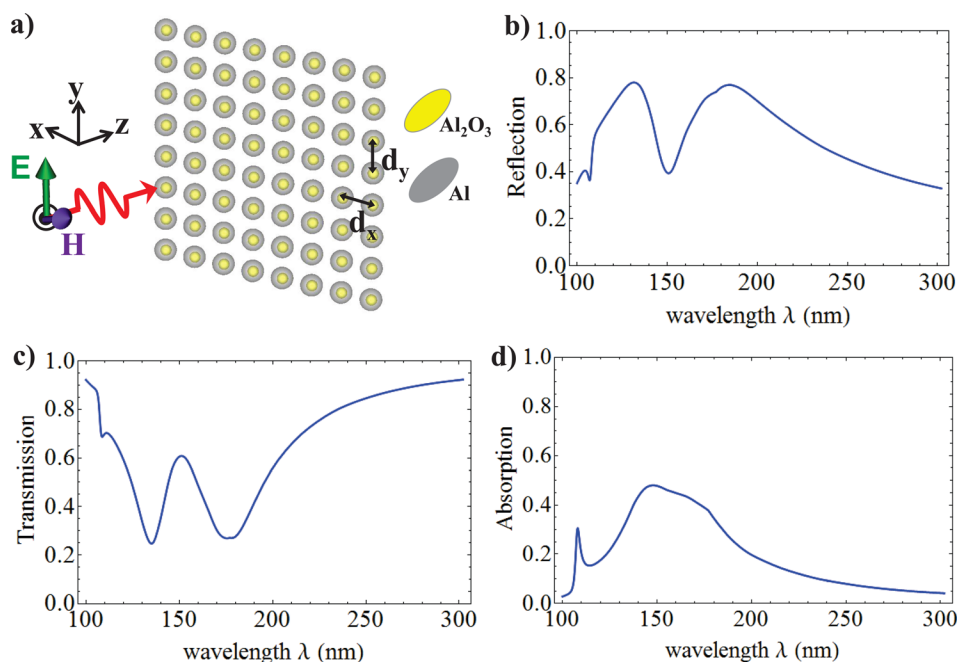


FIG. 4. (a) An infinite periodic array of composite nanoparticles with geometry, parameters and dimensions as in Fig. 1. The periodicity is chosen to be  $d_x = d_y = 2.5a = 21.25$  nm. Amplitude of (b) reflection, (c) transmission, and (d) absorption coefficients of the metasurface shown in panel (a).

consider next an array of composite nanoparticles, in which the effects of interference between radiated fields may be tailored at will. In Fig. 4(a), we show a planar array of the proposed plasmonic nanoparticles, which effectively realizes a quasi-homogeneous planar “metasurface.”<sup>29,30</sup> The nanoparticles have parameters, geometry and dimensions as in Fig. 1 and are arranged in a square lattice with periodicity  $dx = dy = 2.5a$ , where  $a$  is the outer radius of each nanoparticle. Transmission and reflection coefficients of this planarized infinite array are calculated with a fast converging summation,<sup>34</sup> which takes into account the full dynamic coupling among nanoparticles. The amplitude of the resulted reflection and transmission coefficients are plotted in Figs. 4(b) and 4(c), respectively. The proposed “UV-metasurface” provides sharp Fano transmission and reflection features at deep-UV frequencies, similar to the scattering response of the single nanoparticle shown in Fig. 1(a). It is interesting that the transmission signature resembles electromagnetic-induced-transparency (EIT) scattering patterns,<sup>35,36</sup> with the relevant differences that it is based here on purely dipolar resonances, providing more robustness to loss, and it arises at deep-UV frequencies. We have verified that in the limit of weak coupling, the Fano resonance of the finite array tends to the one of an isolated nanoparticle, as long as the interparticle distance is subwavelength, and grating effects are not present.

Finally, the absorption of the proposed UV nanodevice is calculated from the transmission and reflection coefficients using power conservation, and it is plotted in Fig. 4(d). Almost 50% of the total absorption is interestingly achieved in a deep-UV frequency window. This behavior is ideal towards the realization of deep-UV photodetectors and solar blinds, for which we need to efficiently isolate the UV frequencies from the impinging solar radiation spectrum. Similar performance will be obtained in case the metasurface is embedded in different background media, as demonstrated in Fig. 2. Numerous other applications may be envisioned based on the proposed UV-metasurfaces, such as non-line-

of-sight communications<sup>37</sup> with such short-wavelength radiation, and efficient UV optical filters independent of background variations may be designed based on the proposed concepts.

To conclude, we have explored the design and performance of a core-shell plasmonic nanoparticle that strongly interacts with the impinging radiation at deep-UV frequencies, allowing strong manipulation of the scattering response. Dipolar UV Fano resonances have been demonstrated based on a single subwavelength composite nanoparticle consisting of an aluminum shell surrounding a sapphire core. Realistic Ohmic losses and the natural oxidization of Al have been taken into full account in our calculations. The described UV scattering response may be tuned to a large degree by altering the size and shape of the structure, providing additional flexibility in the design of the proposed UV optical filters. The collective response of a planar metasurface composed of an array of the proposed plasmonic nanoparticles has been shown to exhibit sharp UV Fano and EIT features in the reflection and transmission coefficients, which may lead to the realization of integrated planarized UV nanodevices with filtering effects. Moreover, the metasurface has been found to achieve almost 50% of absorption in a deep-UV frequency window, an interesting feature, in particular, for energy harvesting and defense applications. The proposed Fano scattering features have been found to be very robust to different dielectric background media. In conclusion, we believe that our findings may extend the reach of plasmonic Fano resonances and other anomalous effects to deep-UV wavelengths. Our results prove that aluminum is an ideal material to sustain localized plasmons at UV frequencies and may lead to the realization of efficient UV plasmonic devices and nanocircuits.

This work has been partially supported by the ARO STTR project “Dynamically Tunable Metamaterials,” AFOSR with the YIP Award No. FA9550-11-1-0009 and the ONR MURI Grant No. N00014-10-1-0942.

- <sup>1</sup>M. L. Brongersma and V. M. Shalaev, *Science* **328**, 440–441 (2010).
- <sup>2</sup>J. A. Schuller, E. S. Barnard, W. Cai, Y. C. Jun, J. S. White, and M. L. Brongersma, *Nature Mater.* **9**, 193–204 (2010).
- <sup>3</sup>B. Luk'yanchuk, N. I. Zheludev, S. A. Maier, N. J. Halas, P. Nordlander, H. Giessen, and C. Chong, *Nature Mater.* **9**, 707 (2010).
- <sup>4</sup>F. Hao, Y. Sonnefraud, P. V. Dorpe, S. A. Maier, N. J. Halas, and P. Nordlander, *Nano Lett.* **8**, 3983 (2008).
- <sup>5</sup>J. A. Fan, C. Wu, K. Bao, J. Bao, R. Bardhan, N. J. Halas, V. N. Manoharan, P. Nordlander, G. Shvets, and F. Capasso, *Science* **328**, 1135 (2010).
- <sup>6</sup>A. E. Miroshnichenko, S. Flach, and Y. S. Kivshar, *Rev. Mod. Phys.* **82**, 2257 (2010).
- <sup>7</sup>C. Wu, A. B. Khanikaev, R. Adato, N. Arju, A. A. Yanik, H. Altug, and G. Shvets, *Nature Mater.* **11**, 69 (2012).
- <sup>8</sup>S. Mukherjee, H. Sobhani, J. B. Lassiter, R. Bardhan, P. Nordlander, and N. J. Halas, *Nano Lett.* **10**, 2694 (2010).
- <sup>9</sup>D. Wu, S. Jiang, and X. Liu, *J. Phys. Chem. C* **115**, 23797 (2011).
- <sup>10</sup>C. Argyropoulos, P. Y. Chen, F. Monticone, G. D'Aguanno, and A. Alù, *Phys. Rev. Lett.* **108**, 263905 (2012).
- <sup>11</sup>F. Monticone, C. Argyropoulos, and A. Alù, *Sci. Rep.* **2**, 912 (2012).
- <sup>12</sup>F. Monticone, C. Argyropoulos, and A. Alù, *Phys. Rev. Lett.* **110**, 113901 (2013).
- <sup>13</sup>O. Peña-Rodríguez, A. Rivera, M. Campoy-Quiles, and U. Pal, *Nanoscale* **5**, 209–216 (2013).
- <sup>14</sup>A. Boltasseva and H. Atwater, *Science* **331**, 290–291 (2011).
- <sup>15</sup>G. V. Naik, J. Kim, and A. Boltasseva, *Opt. Mater. Express* **1**, 1090 (2011).
- <sup>16</sup>M. Castro-Lopez, D. Brinks, R. Sapienza, and N. F. van Hulst, *Nano Lett.* **11**, 4674–4678 (2011).
- <sup>17</sup>N. Mattiucci, G. D'Aguanno, H. O. Everitt, J. V. Foreman, J. M. Callahan, M. C. Buncick, and M. J. Bloemer, *Opt. Express* **20**, 1868–1877 (2012).
- <sup>18</sup>K. Jha, S. Z. Ahmed, M. Agio, Y. Ekinici, and J. F. Löffler, *J. Am. Chem. Soc.* **134**, 1966–1969 (2012).
- <sup>19</sup>M. W. Knight, L. Liu, Y. Wang, L. Brown, S. Mukherjee, N. S. King, H. O. Everitt, P. Nordlander, and N. J. Halas, *Nano Lett.* **12**, 6000–6004 (2012).
- <sup>20</sup>M. H. Chowdhury, K. Ray, S. K. Gray, J. Pond, and J. R. Lakowicz, *Anal. Chem.* **81**, 1397–1403 (2009).
- <sup>21</sup>J. Lin, A. Mohammadizadeh, A. Neogi, H. Morkoc, and M. Ohtsu, *Appl. Phys. Lett.* **97**, 221104 (2010).
- <sup>22</sup>Q. Q. Gan, L. C. Zhou, V. Dierolf, and F. J. Bartoli, *IEEE Photon. J.* **1**, 245–253 (2009).
- <sup>23</sup>S. Butun, N. A. Cinel, and E. Ozbay, *Opt. Express* **20**, 2649–2656 (2012).
- <sup>24</sup>T. F. Villesen, C. Uhrenfeldt, B. Johansen, J. L. Hansen, H. U. Ulriksen, and A. N. Larsen, *Nanotechnology* **23**, 085202 (2012).
- <sup>25</sup>C. F. Bohren and D. R. Huffman, *Absorption and Scattering of Light by Small Particles* (Wiley, New York, 1983).
- <sup>26</sup>E. D. Palik, *Handbook of Optical Constants of Solids* (Academic Press, New York, 1985).
- <sup>27</sup>A. Alù and N. Engheta, *Phys. Rev. E* **72**, 016623 (2005).
- <sup>28</sup>A. Alù and N. Engheta, *Phys. Rev. Lett.* **102**, 233901 (2009).
- <sup>29</sup>P. Y. Chen and A. Alù, *Phys. Rev. B* **82**, 235405 (2010).
- <sup>30</sup>P. Y. Chen, C. Argyropoulos, and A. Alù, *Nanophotonics* **1**, 221–233 (2012).
- <sup>31</sup>C. Argyropoulos, P. Y. Chen, G. D'Aguanno, N. Engheta, and A. Alù, *Phys. Rev. B* **85**, 045129 (2012).
- <sup>32</sup>R. K. Hart, *Proc. R. Soc. London* **236**, 68 (1956).
- <sup>33</sup>H. P. Godard, *J. Electrochem. Soc.* **114**, 354 (1967).
- <sup>34</sup>P. A. Belov and C. R. Simovski, *Phys. Rev. E* **72**, 026615 (2005).
- <sup>35</sup>S. Zhang, D. A. Genov, Y. Wang, M. Liu, and X. Zhang, *Phys. Rev. Lett.* **101**, 047401 (2008).
- <sup>36</sup>N. Liu, T. Weiss, M. Mesch, L. Langguth, U. Eigenthaler, M. Hirscher, C. Sonnichsen, and H. Giessen, *Nano Lett.* **10**, 1103–1107 (2010).
- <sup>37</sup>Z. Xu and B. M. Sadler, *IEEE Commun. Mag.* **46**, 67–73 (2008).